This is an open access article published under an ACS AuthorChoice License, which permits copying and redistribution of the article or any adaptations for non-commercial purposes.

Biochemistry

Article

Cite This: Biochemistry 2019, 58, 2160−2166

pubs.acs.org/biochemistry

Rapid Deorphanization of Human Olfactory Receptors in Yeast

Emily A. Yasi,[†] Sara L. Eisen,[†] Hanfei Wang,[†] Widianti Sugianto,[†] Anita R. Minniefield,[†] Kaitlyn A. Hoover,[†] Paul J. Branham,[†] and Pamela Peralta-Yahya*[,†,‡]

[†]School of Chemistry and Biochemistry, Georgia Institute of Technology, Atlanta, Georgia 30332, United States

[‡]School of Chemical and Biomolecular Engineering, Georgia Institute of Technology, Atlanta, Georgia 30332, United States

Supporting Information

ABSTRACT: Olfactory receptors are ectopically expressed (exORs) in more than 16 different tissues. Studying the role of exORs is hindered by the lack of known ligands that activate these receptors. Of particular interest are exORs in the colon, the section of the gastrointestinal tract with the greatest diversity of microbiota where ORs may be participating in host−microbiome communication. Here, we leverage a G-protein-coupled receptor (GPCR)-based yeast sensor strain to generate sensors for seven ORs highly expressed in the colon. We screen the seven colon ORs against 57 chemicals likely to bind ORs in olfactory tissue. We successfully deorphanize two colon exORs for the first time, OR2T4 and OR10S1, and find alternative ligands for OR2A7. The same OR deorphanization workflow can be applied to the deorphanization of other ORs and GPCRs in general. Identification of ligands for OR2T4, OR10S1, and OR2A7 will enable the study of these ORs in the colon. Additionally, the colon OR-based sensors will enable the elucidation of endogenous colon metabolites that activate these receptors. Finally, deorphanization of OR2T4 and OR10S1 supports studies of the neuroscience of olfaction.

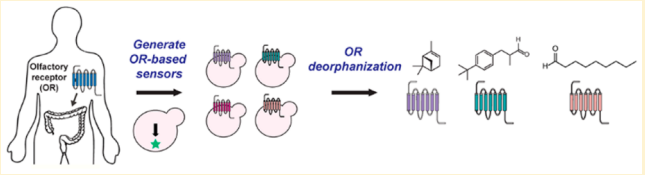

Olfactory receptors (ORs) make up the largest group of G-protein-coupled receptors (GPCRs) and are used by organisms to sense their chemical environment.[1] Rather than binding a single chemical, ORs bind a range of chemicals with different affinities.[2] Identification of ligands that activate orphan ORs remains a challenging process.[3] To date, only 10% of the approximately 400 human ORs have known ligands.[3,4] Both experimental and computational approaches have been applied to OR deorphanization. Among the most large-scale ones is the use of a mammalian-based OR assay to screen 394 human ORs against 73 chemicals to deorphanize 18 ORs.[5,6] Computational approaches have been used to generate machine learning algorithms by virtually screening hundreds of chemicals against ORs with known ligands, yet the algorithms have failed to deorphanize ORs.[7]

More than 20% of the human ORs are also expressed ectopically outside the olfactory tissue,[8,9] and their function in these tissues is just starting to be elucidated. OR1D2 expression in the testis has been implicated in chemotaxis;[10] OR51E2 expression in the kidney mediates renin secretion,[11] and OR151E1 and OR51E2 in the colon respond to short-chain fatty acids[11−14] likely produced by gut microbiota leading to changes in gene expression.[13] The key to studying the role of ectopically expressed ORs (exORs) and the identification of endogenous ligands present in the tissues in which they are expressed is the availability of "synthetic ligands" that activate these receptors in the laboratory. To date, nine of the 84 ectopically expressed human ORs have known ligands.[10−18]

In the human colon, nine ORs are expressed with high confidence: OR10S1, OR2A7, OR2A42, OR2L13, OR2T4, OR2W3, OR51B5, OR51E1, and OR51E2.[9] The role of OR51E2[14] and OR51E1[19] in the colon has been well studied. Synthetic ligands for OR51B5 (isononyl alcohol[17]), OR2A7 (cyclohexyl salicylate[20]), and OR2W3 (nerol[18]) have been reported. The other four ORs (OR10S1, OR2A42, OR2L13, and OR2T4) remain orphans. Deorphanization of these four ORs and finding alternative ligands for OR51B5, OR2A7, and OR2W3 would help to elucidate the role of ORs in the colon. Additionally, deorphanization of OR10S1, OR2A42, OR2L13, and OR2T4 would aid in the studies of the neuroscience of olfaction.

Here, we develop a workflow for the rapid deorphanization of olfactory receptors and apply it to the deorphanization of human ORs expressed in the colon (Figure 1A). Specifically, we leverage a previously engineered GPCR-based yeast sensor strain[21] (Figure 1B) to generate seven colon exOR sensors. We screen each of these colon ORs against a 57-member chemical panel to successfully deorphanize two receptors, OR2T4 and OR10S1, and identify two alternative ligands for OR2A7. The OR deorphanization workflow can be readily applied to the deorphanization of other ORs. The yeast-based OR assay is faster than its mammalian cell counterpart due to the shortened doubling time and nonrequirement of cell passage. In addition, yeast-based OR sensors can be stored for up to a month at 4 °C before use. The newly identified ligands for OR2T4, OR10S1, and OR2A7 now allow for the elucidation of the role of these

Received: November 21, 2018
Revised: March 25, 2019
Published: April 12, 2019

© 2019 American Chemical Society

DOI: 10.1021/acs.biochem.8b01208
Biochemistry 2019, 58, 2160−2166

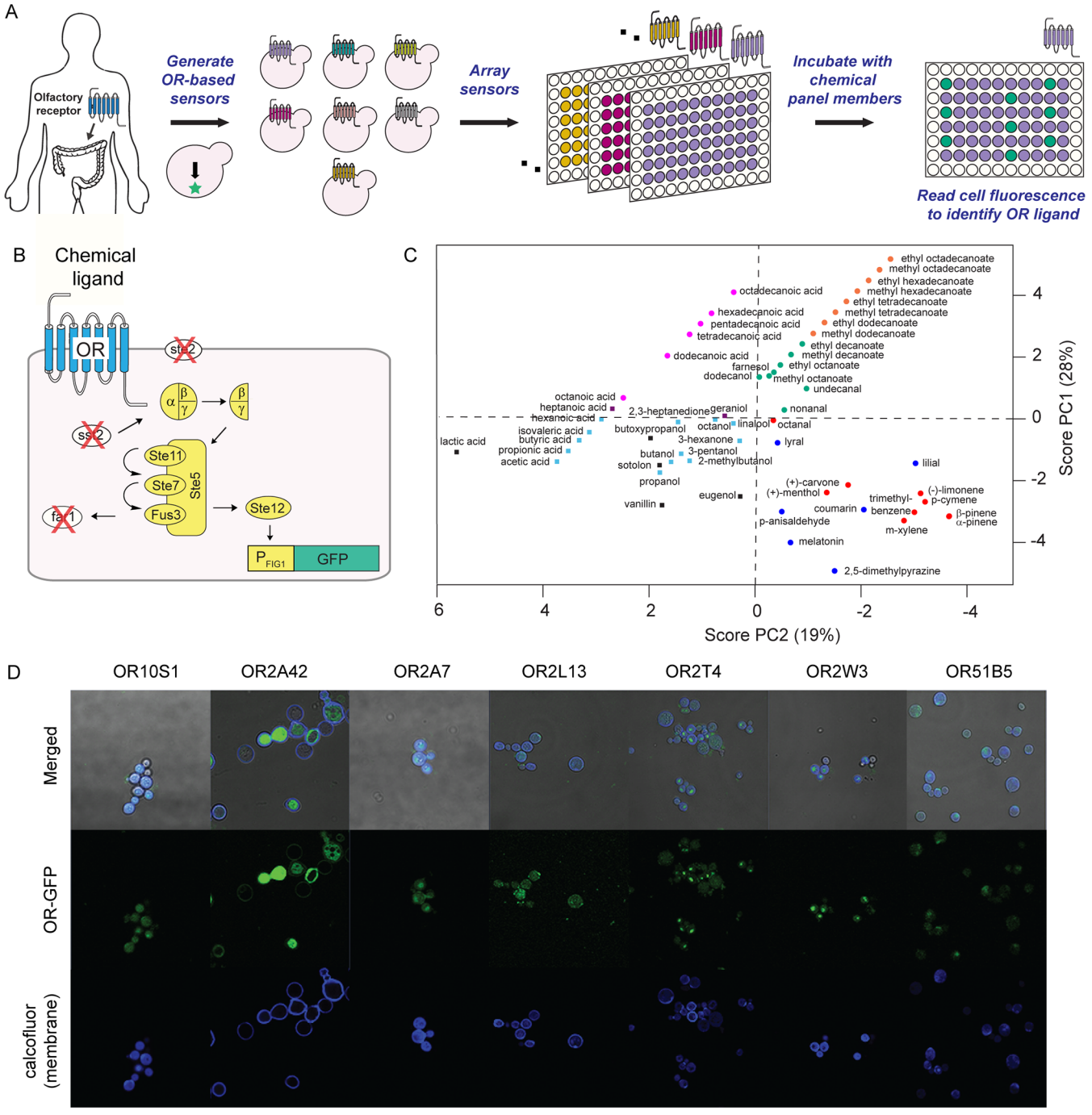

Figure 1. Ectopically expressed olfactory receptor (exOR) sensors and the chemical panel. (A) OR deorphanization workflow. (B) Yeast-based OR sensor. OR (blue) is expressed in a yeast sensor strain that links receptor activation to green fluorescent protein (GFP). (C) Principle component analysis of the 57-member chemical panel. Chemical Spaces (CS): CS1, red dot; CS2, green dot; CS3, blue dot; CS4, orange dot; CS5, purple square; CS6, light blue square; CS7, pink dot; CS8, black square. (D) Localization of human ORs when expressed in yeast.

ORs in the colon. The OR high-throughput screening assay enables the elucidation of endogenous OR ligands in the colon.

MATERIALS AND METHODS

Principle Component Analysis for the Chemical Panel. Simplified molecular-input line-entry system (SMILES) codes for the 57 chemicals in the panel were obtained from PubChem and used as inputs to Instant JChem (ChemAxon) to acquire information about 23 descriptors. Eight descriptors were chemical functional groups, and 15 descriptors were from a method by Wenderski et al.[22] The principle components (PCs) were calculated using Solo Eigenvector (Eigenvector Research). Three PCs, which encompass 63% cumulative variance, were selected by evaluating eigenvalues. PC scores exported from Solo were used to create scatter plots in MATLAB.

Strains and Plasmids. Human olfactory receptors OR2A4, OR2W3, OR2T4, OR51B5, OR2L13, OR10S1, and OR2A7 were codon optimized for *Saccharomyces cerevisiae* and commercially synthesized. ORs were cloned into pKM111 at *Bam*HI/*Sac*II sites via Gibson assembly to create pHW3, pHW6, pHW7, pHW18, pPB8, pHW20, and pHW21,

DOI: 10.1021/acs.biochem.8b01208
Biochemistry 2019, 58, 2160−2166

respectively. The sequences of the plasmids were verified using primers EY46 and HW12. To construct the OR-based sensors, pHW3, pHW6, pHW7, pHW18, pPB8, pHW20, or pHW21 was co-transformed with pRS415-P_{FIG1}-eGFP-Leu2 (pKM586) into yeast sensor strain PPY140[21] (W303 Δ*far1,* Δ*ste2,* Δ*sst2*) to generate PPY1801−1807. To construct the control strain lacking the OR, PPY140 was co-transformed with pKM586 and an empty vector to generate PPY1800.

To construct OR-GFP fusion plasmids, ORs were amplified from pHW3, pHW6, pHW7, pHW18, pPB8, pHW20, and pHW21 using primer HW1 with HW4, HW7, HW8, HW9, PB89, PB116, and PB118, respectively. GFP was amplified from pKM586 using primer HW12 with overlap to ORs with HW15, HW18, HW19, HW20, PB88, PB115, and PB117. ORs and GFP were cloned into pKM111 at *Bam*HI/*Sac*II sites via Gibson assembly to create pHW22, pHW23, pHW30, pHW33, pPB59, pPB60, and pPB54, respectively.

OR Fluorescence Microscopy. Overnight cultures of PPY1949−PPY1955 were used to inoculate 20 mL of SD(H^-) until an OD_{600} of 0.06 was reached. After 18 h at 15 °C (150 rpm), cultures were spun down at 3500 rpm for 10 min and resuspended in 200 μL of SD(H^-). One drop (2 μL) of Calcofluor White Stain (Sigma-Aldrich) and one drop (2 μL) of 10% potassium hydroxide were added to the specimen (2 μL) directly on the slide. Yeast was visualized on a Zeiss LSM 700 confocal microscope using the 63× objective lens. GFP was excited using the 488 nm laser line, and Calcofluor white was excited using the 405 nm line.

Screening ORs with a 57-Member Chemical Panel. Overnight cultures of PPY1801−PPY1807 were used to inoculate 20−40 mL of synthetic complete medium with 2% glucose lacking histidine and leucine [SD(HL^-)] until an OD_{600} of 0.06 was reached. After 18 h at 15 °C (150 rpm), cultures were spun down at 3500 rpm for 10 min and resuspended to an OD_{600} of ≈1 (1/10th of the culture volume). In a 96-well plate, 190 μL of fresh SD(HL^-), 8 μL of the cell suspension, and 2 μL of the solution of the chemical [final chemical concentration of 10 μM, 1% dimethyl sulfoxide (DMSO)] were added. After incubation (4 h, plates covered with Breathe Easy Sealing Membrane, 30 °C, 250 rpm), the GFP fluorescence was read using a Millipore Guava easyCyte HT flow cytometer (λ_{ex} = 488 nm; flow rate of 1.18 μL/s). Samples were run in triplicate. Data from 5000 cells were collected, and 70−95% of viable cells were gated using FlowJo. The geometric mean of the mean fluorescence of the gated cells was used to calculate in Microsoft Excel *p* values using a Student's *t* test with two tails using equal variance to define chemical hits ($p < 0.05$).

OR/Chemical Dose−Response Curves. The same protocol for OR chemical screening was followed. To a test tube were added 4.8 mL of SD(HL^-), 200 μL of the cell suspension, and 50 μL of the chemical (final chemical concentrations of 0−1000 μM, 1% DMSO). After incubation (4 h, plates covered with Breathe Easy Sealing Membrane, 30 °C, 250 rpm), the GFP fluorescence was read using a BD LSR II flow cytometer (488 nm laser line; 515−545 nm filter; FSC, 150 V; SSC, 200 V; FITC, 450 V; FSC threshold, 5000). Samples were run in triplicate. Data from 10000 cells and 70−95% of viable cells were gated using FlowJo. The geometric mean of the mean fluorescence of the gated cells was plotted in OriginPro 2016. Statistically significant points were calculated using Microsoft Excel Student's *t* test with two tails using equal variance. To compare different conditions in a single plot (Figures 3 and 4), the percent GFP expression was calculated using the formula below. First, the percent GFP expression of every data point for each condition was calculated taking into account GFP (AU) for all conditions to be plotted in the same graph. Then, the percent GFP expression was averaged and the standard deviation calculated.

$$\%\ \text{GFP expression} = 100[(\text{GFP}_{\text{sample}} - \text{GFP}_{\text{min}}) / (\text{GFP}_{\text{max}} - \text{GFP}_{\text{min}})]$$

To calculate EC_{50}s, the data in Figures 3 and 4 were fitted to a dose−response equation in OriginPro 2016 using the following formula.

$$y = A_1 + \frac{A_2 - A_1}{1 + 10^{(\log x_0 - x)p}} \qquad \text{EC}_{50} = 10^{\log x_0}$$

RESULTS AND DISCUSSION

Structural Diversity in the 57-Member Chemical Panel. ORs account for 3% of all coding genes in humans[23] and bind a variety of chemicals from terpenes and esters to acids and aldehydes. To identify ligands that activate the seven ORs, we screened them against 57 chemicals likely to bind ORs in olfactory tissue. To understand the structural diversity of the 57 chemicals, each chemical was broken down into 23 descriptors to perform a principle component analysis (Figure 1C). The top three principle components (PCs) account for 63% of the cumulative variance. On the basis of their PC scores, chemicals can be separated into eight chemical spaces (CSs): CS1, cyclic compounds; CS2, medium-chain esters, alcohols, and aldehydes; CS3, aromatic compounds; CS4, long-chain esters; CS5, heptatonic acid and geraniol; CS6, short-chain hydrocarbons with oxygen-containing functional groups; CS7, long-chain acids; CS8, chemicals with at least two oxygen-containing functional groups. The most well represented chemical space is CS6, accounting for 23% of the chemicals in the panel.

Colon OR Sensor Generation. We codon-optimized OR10S1, OR2A7, OR2L13, OR2T4, OR51B5, OR2A42, and OR2W3 for expression in the yeast *S. cerevisiae* and commercially synthesized them. We cloned the ORs under a strong promoter in a high-copy number plasmid and transformed them in the GPCR yeast sensor strain[21] to generate the seven colon OR-based sensors. Incubation of OR2W3 with nerol did not result in a significant increase in the signal after activation (Figure S1). ORs sometimes bind different ligands depending on the G_α subunit to which they are coupling.[24,25] Sometimes, an OR is activated by the same ligand independent of the G_α subunit to which it is coupled, and when it is coupled to G_{olf}, a signal enhancement in observed.[26,27] Nerol was discovered as a ligand for OR2W3 using G_{olf}.[18] In the yeast system, the ORs couple to the native yeast G_α subunit GPA1. It is possible that nerol does not efficiently activate OR2W3 when coupling to GPA1. Cyclohexyl salicylate ($400/mg) and isononyl alcohol ($600/mg) were not readily available and too expensive to be used as synthetic ligands for OR2A7 and OR51B5, respectively. Thus, we set out to identify ligands for all seven ORs. The seven ORs do not have a high degree of sequence identity with the closest sequences being OR2A7 and OR2A42 (71.3%) and the most distant sequences being OR51B5 and OR2L13 (26.2%) (Table S1).

Verification of Colon OR Expression in Yeast. To verify the yeast expression of the seven human ORs, we fused green fluorescent protein (GFP) to the C-terminus of the ORs. The

DOI: 10.1021/acs.biochem.8b01208
Biochemistry 2019, 58, 2160−2166

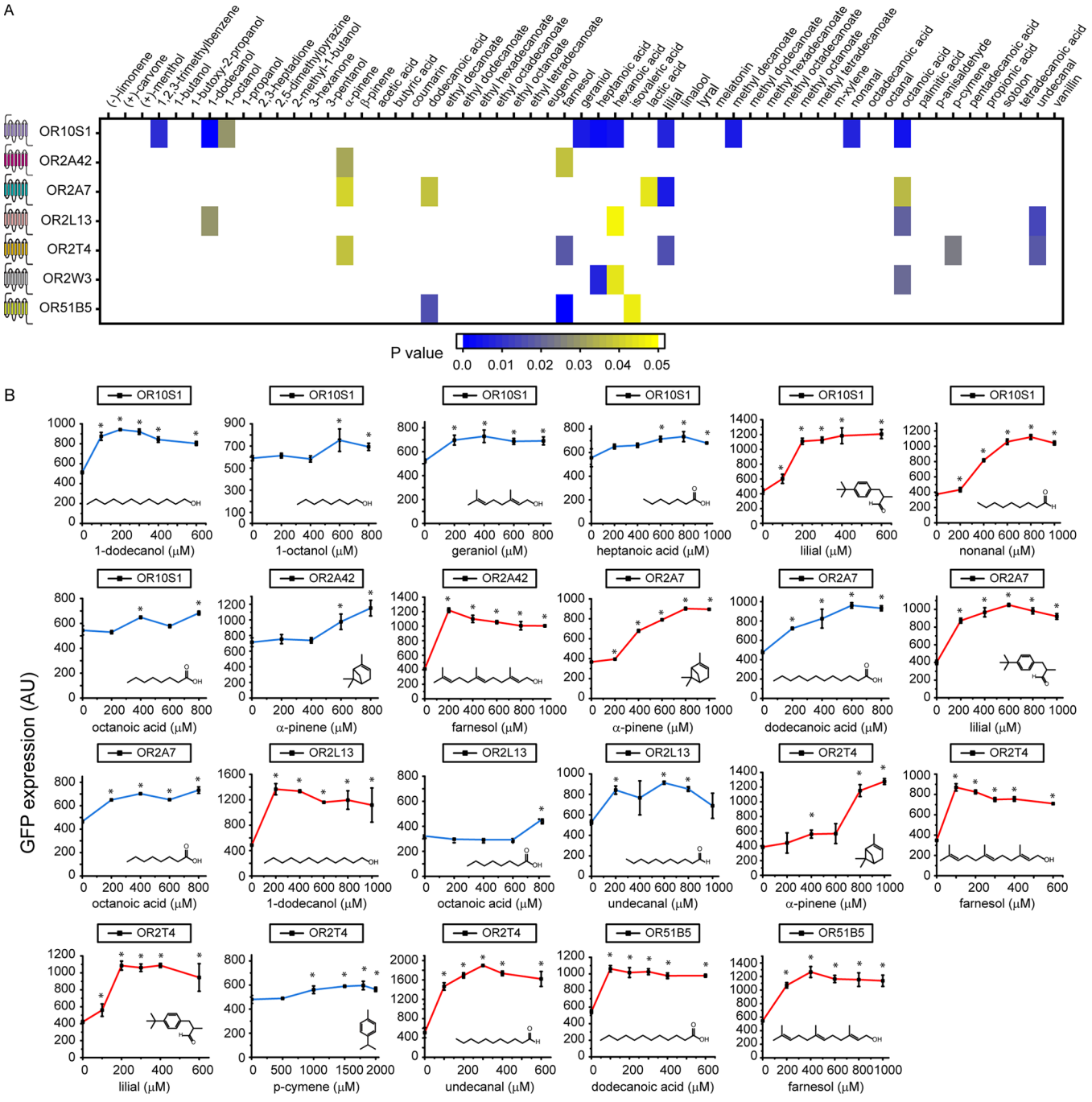

Figure 2. Rapid deorphanization of human olfactory receptors (ORs). (A) Heat map of p values of chemicals leading to a statistically significant increase in the level of GFP expression when compared to the dimethyl sulfoxide (DMSO) control ($p < 0.05$). (B) Dose−response curves of ORs with 23 chemical hits. Blue curves are for chemicals leading to a statistically significant increase in the intensity of the signal after activation. Red curves are for chemicals resulting in a >2-fold increase in the intensity of the signal after activation. Asterisks denote statistically significant increases ($p < 0.05$) in the intensity of the signal after activation when compared to no chemical. Figure S2 shows dose−response curves of the nine OR/chemical pairs that did not result in a statistically larger increase in the intensity of the signal after activation. All measurements were carried out in triplicate, and means ± the standard deviation are shown.

seven ORs are expressed in yeast and could be found at the cell membrane (Figure 1D). The OR expression pattern was sequence-dependent. While OR2A42 was mostly localized to the cell membrane, OR10S1 was expressed throughout yeast. OR2T4 and OR2W3 showed a punctuated pattern, i.e., the ORs had challenges translocating to the membrane, likely accumulating in the endoplasmic reticulum. Of note, the OR sensor strain amplifies the chemical signal detected by the OR; i.e., activation of the OR leads to the activation of a large number of transcription factors that go on to activate GFP expression. Thus, it is not necessary to have a large number of ORs on the cell surface to detect GFP expression.

Rapid Screening of Colon ORs against the 57-Member Chemical Panel. Each OR was screened in triplicate against 57 chemicals and DMSO as a control. Chemicals resulting in a statistically significantly increase in the level of GFP expression

DOI: 10.1021/acs.biochem.8b01208
Biochemistry 2019, 58, 2160−2166

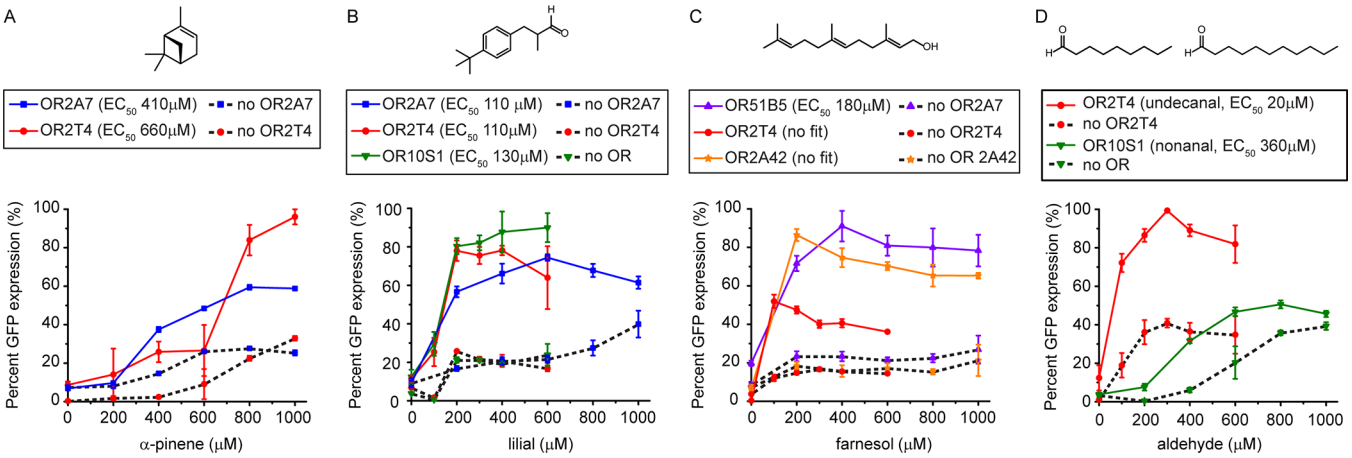

Figure 3. Confirming OR-dependent activation with validated chemicals. Dose−response curves of validated chemicals in the presence (solid lines) and absence (dotted lines) of ORs: (A) OR2A7 and OR2T4 with α-pinene, (B) OR2A7, OR2T4, and OR10S1 with lilial, (C) OR51B5, OR2T4, and OR2A42 with farnesol, and (D) OR2T4 and OR10S1 with undecanal and nonanal, respectively. All measurements were carried out in triplicate, and means ± the standard deviation are shown. Figure S3 shows dose−response curves of three OR/chemical pairs that do not show OR-dependent GFP expression. Table S8 lists R^2 values for dose−response fits.

($p < 0.05$) when compared to the DMSO control were considered hits (Figure 2A). There were a total of 32 chemical hits. OR10S1 had the largest number of hits (10). OR2T4 and OR2A7 had five hits each. OR2A42 had the fewest number of chemical hits (two).

Secondary Screening of OR Chemical Hits. To validate the chemical hits from the rapid screening stage, we determined dose−response curves of the OR/chemical hit pairs (Figure 2B and Figure S2). Chemical hits were validated if at any of the concentrations tested in the dose−response curve there was a statistically significant increase in the signal after activation when compared to the DMSO control. In the case of OR10S1, seven of 10 chemical hits were validated, with lilial and nonanal leading to a >2-fold increase in the signal after activation. All five OR2T4 chemical hits were validated, with α-pinene, farnesol, lilial, and undecanal showing a >2-fold increase in the signal. The two OR2A42 chemical hits were validated, with farnesol resulting in a 2-fold increase in the signal after activation. Four of the five OR2A7 chemical hits were validated, with α-pinene and lilial leading to a >2-fold increase in the signal after activation. In the case of OR2L13, three of the four chemical hits were validated, with dodecanol and undecanal resulting in a >2-fold increase in the signal. Two of the three OR51B5 chemical hits were validated with dodecanoic and farnesol leading to a >2-fold increase in the signal after activation. None of the three OR2W3 chemical hits were validated. Taken together, we validated at least one hit for each OR except for OR2W3. We find multiple hits for some ORs, which is consistent with olfactory receptors' tendency to bind a family of chemicals.

Confirming OR-Dependent GFP Expression. To confirm that the validated chemicals lead to cell fluorescence via OR activation and not an alternative mechanism, we determined dose−response curves of the validated chemicals with a control strain carrying an empty vector in place of the OR and the GFP reporter plasmid (Figure 3 and Figure S3). We focused on OR/chemical pairs resulting in a ≥2-fold increase in the signal after activation: pinene with OR2A7 and OR2T4; lilial with OR2A7, OR2T4, and OR10S1; farnesol with OR51B5, OR2T4, and OR2A52; nonanal with OR10S1; and undecanal with OR2T4. The chemicals inhibit cell growth, but the cells remain at the same optical density as at the start of the experiment (Figure S4). We fitted the OR/chemical pair data to a dose−response equation to calculate EC_{50}s.

To reliably compare the responses of the chemicals, we ran OR and no OR control experiments pairwise on the same day.

Pinene elicits basal GFP expression in the absence of a receptor (Figure 3A). In the presence of pinene, the OR2A7 EC_{50} is 412 μM while the OR2T4 EC_{50} is 659 μM. In the presence of OR2T4, pinene addition results in a 3-fold increase in GFP expression when compared to the no receptor control. In contrast, in the presence of OR2A7, pinene addition results in an only 2.3-fold increase in percent GFP expression when compared to the no receptor control. The maximal level of GFP expression of OR2T4 is 63% higher than that of OR2A7.

Lilial elicits a basal GFP expression that is comparable to that of pinene (Figure 3B). The EC_{50}s of OR2A7 and OR2T4 with lilial are almost indistinguishable at 110 and 107 μM, respectively. Lilial shows a lower chemical potency with OR10S1 with an EC_{50} of 129 μM. Lilial elicits GFP expression with OR10S1, resulting in a 3.8-fold increase in percent GFP expression when compared to the no receptor control.

Farnesol results in a basal GFP expression that is comparable to that seen with pinene and lilial (Figure 3C). The farnesol response obtained in the presence of OR2T4 and OR2A42 could not be fitted to a dose−response equation with the curves resembling an on/off response. The response of OR51B5 to farnesol could be fitted to a dose−response curve, resulting in an EC_{50} of 181 μM, and it has a 3-fold increase in percent GFP expression compared to the no receptor control.

The two aldehydes, undecanal and nonanal, elicit a slightly higher basal GFP expression than pinene, lilial, or farnesol (Figure 3D). Although OR10S1 shows an increase in its signal after activation upon nonanal addition, the no OR control shows a similar increase in GFP expression. In the presence of OR2T4, the addition of undecanal results in a 2.3-fold increase in percent GFP expression when compared to the no receptor control.

Taken together, pinene is a confirmed ligand for OR2A7 and OR2T4, lilial is a confirmed ligand for OR2A7, OR2T4, and OR10S1, while undecanal is a confirmed ligand for OR2T4. Addition of these chemicals does not elicit an increase in the level of OR gene expression when compared to the DMSO control (Figure S5). Thus, the increase in GFP expression is due

DOI: 10.1021/acs.biochem.8b01208
Biochemistry 2019, 58, 2160−2166

to signal transfer and not an increase in the number of olfactory receptors expressed. Farnesol does not result in a dose–response fit with OR2T4 or OR2A42; thus, it is not a ligand for these ORs. Although addition of farnesol to OR51B5 did result in a dose–response fit, the response has an overall on/off behavior (except for the data point at 200 μM farnesol). To test if farnesol generally increases the level of GFP expression in the presence of ORs, we measured the response of OR2W3 and OR2A7 upon addition of farnesol (Figure S6). In the presence of OR2W3 or OR2A7, farnesol elicits GFP expression, yet the data do not fit a dose–response curve. In conclusion, farnesol nonspecifically activates GFP expression in the OR-based sensors.

Understanding the Chemical Activation Profile of OR2A7 and OR2T4. We determined the dose–response curves of OR2A7 and OR2T4 with chemicals that have stereochemistry and substructure different from those of the identified hits, pinene and lilial. Activation of the ORs is dependent on pinene stereochemistry. OR2A7 shows an 18% weaker response with β-pinene than α-pinene, while the response of OR2T4 to β-pinene is similar to the GFP expression of the no OR control (Figure 4A,B). Both OR2T4 and OR2A7 are activated by lilial. We

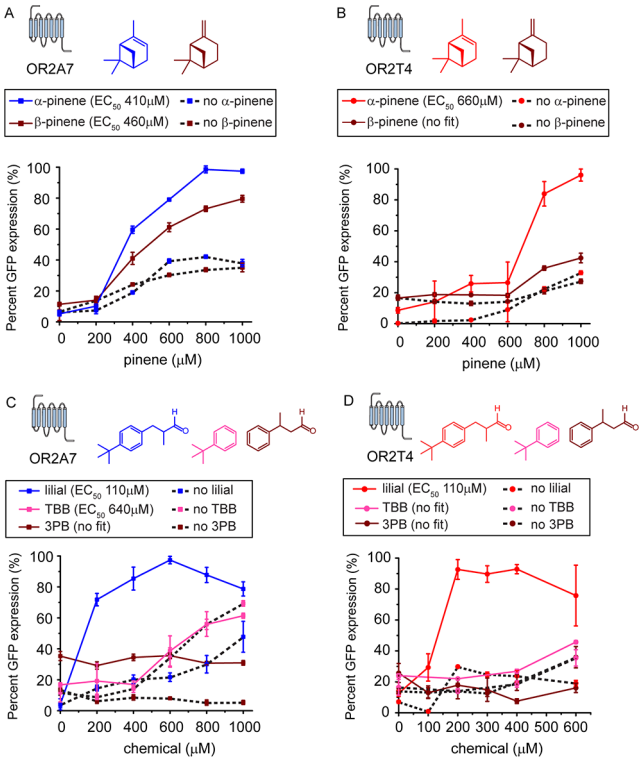

Figure 4. Chemical activation profiles of OR2A7 and OR2T4. Dose–response curves of (A) OR2A7 with α-pinene and β-pinene, (B) OR2T4 with α-pinene and β-pinene, (C) OR2A7 with lilial, 3-phenylbutyraldehyde (3PB), and *tert*-butylbenzene (TBB), and (D) OR2T4 with lilial, 3PB, and TBB, All measurements were carried out in triplicate, and means ± the standard deviation are shown.

probed the activation profile of OR2T4 and OR2A7 with 3-phenylbutyraldehyde (3PB), which retains the aldehyde found in lilial but lacks the *tert*-butyl group, and *tert*-butylbenzene (TBB), which lacks the aldehyde moiety but retains the phenyl and *tert*-butyl groups. We find that to activate OR2T4 and OR2A7, the *tert*-butyl group and the aldehyde side chain are necessary (Figure 4C,D). Although TBB shows an increase in the level of GFP expression at >600 μM, the no receptor control shows a similar increase in the level of GFP expression, making the signal observed not OR dependent.

CONCLUSION

Here, we leveraged a previously engineered GPCR-based yeast sensing strain to generate sensors for seven ORs found in the human colon. Yeast's robustness and rapid doubling time allowed us to quickly screen each of the seven colon ORs against 57 chemicals and deorphanize two receptors, OR2T4 (α-pinene, lilial, and undecanal) and OR10S1 (lilial), and identify two new inexpensive ligands for OR2A7 (α-pinene and lilial). The rapid deorphanization workflow can be repeated to deorphanize other ORs and can be used, in the future, to identify the endogenous ligands of OR2T4, OR10S1, and OR2A7 in the colon. The yeast-based sensor used in this work links the human ORs to GFP expression via yeast G_α subunit GPA1. Sometimes, an OR is activated by different ligands depending on the G_α subunit to which they couple.[24,25] Sometimes, ORs are activated by a ligand independent of the G_α subunit to which it couples, and using G_{olf} enhances the signal.[26,27] In the future, the OR/ligand pairs identified in this work can be coupled to G_{olf} to determine the situation under which they fall. This can be accomplished using the mammalian OR sensor system that expresses G_{olf}[5,28] or by expressing G_{olf} in yeast.

We did not find ligands for OR2A42, OR2L13, OR2W3, or OR51B5. Although these ORs are expressed in yeast, it is possible that they are not coupling to the yeast machinery. Alternatively, ligands for these receptors may not be present among the 57 chemicals tested. Deorphanization of these ORs will likely require the use of G_{olf}/GPA1 fusion protein for improved coupling to the yeast machinery and a larger chemical library against which to screen.

ASSOCIATED CONTENT

Supporting Information

The Supporting Information is available free of charge on the ACS Publications website at DOI: 10.1021/acs.biochem.8b01208.

Materials, methods, and sequences; sequence identities of olfactory receptors expressed in the colon (Table S1); primers (Table S2); plasmids (Table S3); strains (Table S4); chemicals in the chemical panel (Table S5); abbreviations and chemical descriptors used in the principle component analysis (Table S6); chemical space coordinates of the screened chemicals (Table S7); R^2 values for dose–response fits (Table S8); dose–response curve of OR2W3 with nerol (Figure S1); dose–response curves of colon ORs with chemical hits (false positives) (Figure S2); dose–response curves of OR2L13 and OR51B5 with validated chemicals (Figure S3); chemical toxicity to yeast-based OR sensors (Figure S4); changes in olfactory receptor gene expression levels in the presence of chemicals (Figure S5); dose–response curves of OR2A7 and OR2W3 with farnesol (Figure S6); and eigenvalues for principle component determination (Figure S7) (PDF)

AUTHOR INFORMATION

Corresponding Author

*E-mail: pperalta-yahya@chemistry.gatech.edu.

DOI: 10.1021/acs.biochem.8b01208
Biochemistry 2019, 58, 2160–2166

ORCID

Pamela Peralta-Yahya: 0000-0002-0356-2274

Author Contributions

E.Y. and P.P.-Y. conceived and designed the experiments and wrote the manuscript. E.Y., S.E., K.H., A.M., H.W., P.B., and W.S. carried out the experiments. All authors approved the manuscript.

Funding

This work funded by a National Institutes of Health MIRA Award (R35GM124871) to P.P.-Y.

Notes

The authors declare no competing financial interest.

■ ABBREVIATIONS

OR, olfactory receptor; exOR, ectopically expressed olfactory receptor; GPCR, G-protein-coupled receptor; PC, principle component; DMSO, dimethyl sulfoxide; 3PB, 3-phenylbutyraldehyde; TBB, *tert*-butylbenzene.

■ REFERENCES

(1) Spehr, M., and Munger, S. D. (2009) Olfactory receptors: G protein-coupled receptors and beyond. *J. Neurochem. 109*, 1570−1583.

(2) Buck, L. B. (2004) Olfactory receptors and odor coding in mammals. *Nutr. Rev. 62*, S184−S188.

(3) Peterlin, Z., Firestein, S., and Rogers, M. E. (2014) The state of the art of odorant receptor deorphanization: A report from the orphanage. *J. Gen. Physiol. 143*, 527−542.

(4) de March, C. A., Ryu, S., Sicard, G., Moon, C., and Golebiowski, J. (2015) Structure−odour relationships reviewed in the postgenomic era. *Flavour Fragrance J. 30*, 342−361.

(5) Mainland, J. D., Keller, A., Li, Y. R., Zhou, T., Trimmer, C., Snyder, L. L., Moberly, A. H., Adipietro, K. A., Liu, W. L., Zhuang, H., Zhan, S., Lee, S. S., Lin, A., and Matsunami, H. (2014) The missense of smell: functional variability in the human odorant receptor repertoire. *Nat. Neurosci. 17*, 114−120.

(6) Mainland, J. D., Li, Y. R., Zhou, T., Liu, W. L. L., and Matsunami, H. (2015) Human olfactory receptor responses to odorants. *Sci. Data 2*, 150002.

(7) Bushdid, C., de March, C. A., Fiorucci, S., Matsunami, H., and Golebiowski, J. (2018) Agonists of G-Protein-Coupled Odorant Receptors Are Predicted from Chemical Features. *J. Phys. Chem. Lett. 9*, 2235−2240.

(8) Flegel, C., Manteniotis, S., Osthold, S., Hatt, H., and Gisselmann, G. (2013) Expression profile of ectopic olfactory receptors determined by deep sequencing. *PLoS One 8*, No. e55368.

(9) Feldmesser, E., Olender, T., Khen, M., Yanai, I., Ophir, R., and Lancet, D. (2006) Widespread ectopic expression of olfactory receptor genes. *BMC Genomics 7*, 121.

(10) Spehr, M., Gisselmann, G., Poplawski, A., Riffell, J. A., Wetzel, C. H., Zimmer, R. K., and Hatt, H. (2003) Identification of a testicular odorant receptor mediating human sperm chemotaxis. *Science 299*, 2054−2058.

(11) Pluznick, J. L., Protzko, R. J., Gevorgyan, H., Peterlin, Z., Sipos, A., Han, J., Brunet, I., Wan, L. X., Rey, F., Wang, T., Firestein, S. J., Yanagisawa, M., Gordon, J. I., Eichmann, A., Peti-Peterdi, J., and Caplan, M. J. (2013) Olfactory receptor responding to gut microbiota-derived signals plays a role in renin secretion and blood pressure regulation. *Proc. Natl. Acad. Sci. U. S. A. 110*, 4410−4415.

(12) Leja, J., Essaghir, A., Essand, M., Wester, K., Oberg, K., Tötterman, T. H., Lloyd, R., Vasmatzis, G., Demoulin, J. B., and Giandomenico, V. (2009) Novel markers for enterochromaffin cells and gastrointestinal neuroendocrine carcinomas. *Mod. Pathol. 22*, 261−272.

(13) Priori, D., Colombo, M., Clavenzani, P., Jansman, A. J., Lallès, J. P., Trevisi, P., and Bosi, P. (2015) The Olfactory Receptor OR51E1 Is Present along the Gastrointestinal Tract of Pigs, Co-Localizes with Enteroendocrine Cells and Is Modulated by Intestinal Microbiota. *PLoS One 10*, No. e0129501.

(14) Fleischer, J., Bumbalo, R., Bautze, V., Strotmann, J., and Breer, H. (2015) Expression of odorant receptor Olfr78 in enteroendocrine cells of the colon. *Cell Tissue Res. 361*, 697−710.

(15) Zhang, X., Bedigian, A. V., Wang, W., and Eggert, U. S. (2012) G protein-coupled receptors participate in cytokinesis. *Cytoskeleton 69*, 810−818.

(16) Veitinger, T., Riffell, J. R., Veitinger, S., Nascimento, J. M., Triller, A., Chandsawangbhuwana, C., Schwane, K., Geerts, A., Wunder, F., Berns, M. W., Neuhaus, E. M., Zimmer, R. K., Spehr, M., and Hatt, H. (2011) Chemosensory Ca2+ Dynamics Correlate with Diverse Behavioral Phenotypes in Human Sperm. *J. Biol. Chem. 286*, 17311−17325.

(17) Manteniotis, S., Wojcik, S., Göthert, J. R., Dürig, J., Dührsen, U., Gisselmann, G., and Hatt, H. (2016) Deorphanization and characterization of the ectopically expressed olfactory receptor OR51B5 in myelogenous leukemia cells. *Cell Death Discovery 2*, 16010.

(18) Flegel, C., Vogel, F., Hofreuter, A., Schreiner, B. S., Osthold, S., Veitinger, S., Becker, C., Brockmeyer, N. H., Muschol, M., Wennemuth, G., Altmüller, J., Hatt, H., and Gisselmann, G. (2016) Characterization of the Olfactory Receptors Expressed in Human Spermatozoa. *Front. Mol. Biosci. 2*, 73.

(19) Fujita, Y., Takahashi, T., Suzuki, A., Kawashima, K., Nara, F., and Koishi, R. (2007) Deorphanization of Dresden G protein-coupled receptor for an odorant receptor. *J. Recept. Signal Transduction Res. 27*, 323−334.

(20) Tsai, T., Veitinger, S., Peek, I., Busse, D., Eckardt, J., Vladimirova, D., Jovancevic, N., Wojcik, S., Gisselmann, G., Altmüller, J., Ständer, S., Luger, T., Paus, R., Cheret, J., and Hatt, H. (2017) Two olfactory receptors-OR2A4/7 and OR51B5-differentially affect epidermal proliferation and differentiation. *Exp. Dermatol. 26*, 58−65.

(21) Mukherjee, K., Bhattacharyya, S., and Peralta-Yahya, P. (2015) GPCR-Based Chemical Biosensors for Medium-Chain Fatty Acids. *ACS Synth. Biol. 4*, 1261−1269.

(22) Wenderski, T. A., Stratton, C. F., Bauer, R. A., Kopp, F., and Tan, D. S. (2015) Principal Component Analysis as a Tool for Library Design: A Case Study Investigating Natural Products, Brand-Name Drugs, Natural Product-Like Libraries, and Drug-Like Libraries. *Methods Mol. Biol. 1263*, 225−242.

(23) Zhang, X., De la Cruz, O., Pinto, J. M., Nicolae, D., Firestein, S., and Gilad, Y. (2007) Characterizing the expression of the human olfactory receptor gene family using a novel DNA microarray. *Genome Biol. 8*, R86.

(24) Shirokova, E., Schmiedeberg, K., Bedner, P., Niessen, H., Willecke, K., Raguse, J. D., Meyerhof, W., and Krautwurst, D. (2005) Identification of specific ligands for orphan olfactory receptors. G protein-dependent agonism and antagonism of odorants. *J. Biol. Chem. 280*, 11807−11815.

(25) Ukhanov, K., Bobkov, Y., Corey, E. A., and Ache, B. W. (2014) Ligand-selective activation of heterologously-expressed mammalian olfactory receptor. *Cell Calcium 56*, 245−256.

(26) Minic, J., Persuy, M. A., Godel, E., Aioun, J., Connerton, I., SAlesse, R., and Pajot-Augy, E. (2005) Functional expression of olfactory receptors in yeast and development of a bioassay for odorant screening. *FEBS J. 272*, 524−537.

(27) Fukutani, Y., Nakamura, T., Yorozu, M., Ishii, J., Kondo, A., and Yohda, M. (2012) The N-terminal replacement of an olfactory receptor fort he development of a yeast-based biomimetic odor sensor. *Biotechnol. Bioeng. 109*, 205−212.

(28) Zhuang, H., and Matsunami, H. (2008) Evaluating cell-surface expression and measuring activation of mammalian odorant receptors in heterologous cells. *Nat. Protoc. 3*, 1402−1413.

DOI: 10.1021/acs.biochem.8b01208
Biochemistry 2019, 58, 2160−2166